

Thermal Phase Mixing During First Order Phase Transitions

Julian Borrill¹⁾ and Marcelo Gleiser^{*2)}

¹⁾ *Blackett Laboratory, Imperial College*

Prince Consort Road, London SW7 2BZ, UK

²⁾ *Department of Physics and Astronomy, Dartmouth College*

Hanover, NH 03755, USA

(IMPERIAL/TP/93-94/58 DART-HEP-94/06 September 1994)

Abstract

The dynamics of first order phase transitions are studied in the context of (3+1)-dimensional scalar field theories. Particular attention is paid to the question of quantifying the strength of the transition, and how ‘weak’ and ‘strong’ transitions have different dynamics. We propose a model with two available low temperature phases separated by an energy barrier so that one of them becomes metastable below the critical temperature T_c . The system is initially prepared in this phase and is coupled to a thermal bath. Investigating the system at its critical temperature, we find that ‘strong’ transitions are characterized by the system remaining localized within its initial phase, while ‘weak’ transitions are characterized by considerable phase mixing. Always at T_c , we argue that the two regimes are themselves separated by a (second order) phase transition, with an order parameter given by the fractional population difference between the two phases and a control parameter given by the strength of the scalar field’s quartic self-coupling constant. We obtain a Ginzburg-like criterion to distinguish between ‘weak’ and ‘strong’ transitions, in agreement with previous results in (2+1)-dimensions.

*NSF Presidential Faculty Fellow

I. INTRODUCTION

The fact that the gauge symmetries describing particle interactions can be restored at high enough temperatures has led, during the past 15 years or so, to an active research program on the possible implications that this symmetry restoration might have had to the physics of the very early Universe. One of the most interesting and popular possibilities is that during its expansion the Universe underwent a series of phase transitions, as some higher symmetry group was successively broken into products of smaller groups, up to the present standard model described by the product $SU(3)_C \otimes SU(2)_L \otimes U(1)_Y$. Most models of inflation and the formation of topological (and nontopological defects) are well-known consequences of taking the existence of cosmological phase transitions seriously [1].

One of the motivations of the present work comes from the possibility that the baryon asymmetry of the Universe could have been dynamically generated during a first order electroweak phase transition [2]. As is by now clear, a realistic calculation of the net baryon number produced during the transition is a formidable challenge. We probably must invoke physics beyond the standard model (an exciting prospect for most people) [3], push perturbation theory to its limits (and beyond, due to the nonperturbative nature of magnetic plasma masses that regulate the perturbative expansion in the symmetric phase), and we must deal with nonequilibrium aspects of the phase transition. Here we will focus on the latter problem, as it seems to us to be the least discussed of the pillars on which most baryon number calculations are built upon. To be more specific, we can separate the nonequilibrium aspects of the phase transition into two main subdivisions. If the transition proceeds by bubble nucleation, we can study the propagation of bubbles in the hot plasma and the transport properties of particles through the bubble wall. A considerable amount of work has been devoted to this issue, and the reader can consult

the works of Ref. [4] for details. These works assume that homogeneous nucleation theory is adequate to investigate the evolution of the phase transition, at least for the range of parameters of interest in the particular model being used to generate the baryon asymmetry. This brings us to the second important aspect of the nonequilibrium dynamics of first order phase transitions, namely the validity of homogeneous nucleation theory to describe the approach to equilibrium. This is the issue addressed in the present work.

Nucleation theory is a well-studied, but far from exhausted, subject. Since the pioneering work of Becker and Döring on the nucleation of droplets in supercooled vapor [5], the study of first order phase transitions has been of interest to investigators in several fields, from meteorology and materials science to quantum field theory and cosmology. Phenomenological field theories were developed by Cahn and Hilliard and by Langer [6,7] in the context of coarse-grained time-dependent Ginzburg-Landau models, in which an expression for the decay rate per unit volume was obtained by assuming a steady-state probability current flowing through the saddle-point of the free-energy functional [7,8]. The application of metastable decay to quantum field theory was initiated by Voloshin, Kobzarev, and Okun [9], and soon after put onto firmer theoretical ground by Coleman and Callan [10]. The generalization of these results for finite temperature field theory was first studied by Linde [11], and has been the focus of much recent attention [12].

The crucial ingredient in the evaluation of the decay rate is the computation of the imaginary part of the free energy. As shown by Langer [7], the decay rate \mathcal{R} is proportional to the imaginary part of the free energy \mathcal{F} ,

$$\mathcal{R} = \frac{|E_-|}{\pi T} \text{Im}\mathcal{F} , \quad (1)$$

where E_- is the negative eigenvalue related to metastability, which depends on nonequilibrium aspects of the dynamics, such as the coupling strength to the thermal bath. Since $\mathcal{F} = -T\ln Z$, where Z is the partition function, the computation for the rate boils down

to the evaluation of the partition function for the system comprised of bubbles of the lower energy phase inside the metastable phase. For a dilute gas of bubbles only, the partition function for several bubbles is given by [13,7],

$$\begin{aligned} Z &\simeq Z(\varphi_f) + Z(\varphi_f) \left[\frac{Z(\varphi_b)}{Z(\varphi_f)} \right] + Z(\varphi_f) \frac{1}{2!} \left[\frac{Z(\varphi_b)}{Z(\varphi_f)} \right]^2 + \dots \\ &\simeq Z(\varphi_f) \exp \left[\frac{Z(\varphi_b)}{Z(\varphi_f)} \right], \end{aligned} \quad (2)$$

where φ_f is the metastable vacuum field configuration and φ_b is the bubble configuration, the bounce solution to the $O(3)$ -symmetric Euclidean equation of motion. We must evaluate the partition functions above. This is done by the saddle-point method, expanding the scalar field $\phi(\mathbf{x}, \tau)$, such that $\phi(\mathbf{x}, \tau) \rightarrow \varphi_f + \zeta(\mathbf{x}, \tau)$ for $Z(\varphi_f)$, and $\phi(\mathbf{x}, \tau) \rightarrow \varphi_b(\mathbf{x}) + \eta(\mathbf{x}, \tau)$ for $Z(\varphi_b)$, where $\zeta(\mathbf{x}, \tau)$ and $\eta(\mathbf{x}, \tau)$ are small fluctuations about equilibrium. Skipping details [12], up to one-loop order one obtains for the ratio of partition functions, $\frac{Z(\varphi_b)}{Z(\varphi_f)}$,

$$\frac{Z(\varphi_b)}{Z(\varphi_f)} \stackrel{1\text{-loop order}}{\simeq} \left[\frac{\det(-\square_E + V''(\varphi_b))_\beta}{\det(-\square_E + V''(\varphi_f))_\beta} \right]^{-\frac{1}{2}} e^{-\Delta S}, \quad (3)$$

where $[\det(M)_\beta]^{-\frac{1}{2}} \equiv \int D\eta \exp \left\{ - \int_0^\beta d\tau \int d^3x \frac{1}{2} \eta [M] \eta \right\}$ and $\Delta S = S_E(\varphi_b) - S_E(\varphi_f)$ is the difference between the Euclidean actions for the field configurations φ_b and φ_f . [Note that $S_E(\varphi)$, and hence ΔS , does not include any temperature corrections.] Thus, the free energy of the system is,

$$\mathcal{F} = -T \left[\frac{\det(-\square_E + V''(\varphi_b))_\beta}{\det(-\square_E + V''(\varphi_f))_\beta} \right]^{-\frac{1}{2}} e^{-\Delta S}. \quad (4)$$

We are briefly reproducing this computation here because we want to stress the importance of the assumptions built into it. First, that the partition function is given by equation 2 within the dilute gas approximation, and second, that the partition function is evaluated assuming *small* fluctuations about the homogeneous metastable state φ_f . It is clear that for situations in which there are large amplitude fluctuations about the

metastable equilibrium state the above formula must break down. Thus the breakdown of the expression for the rate is intimately connected with the question of how well-localized the system is about the metastable state as the temperature drops below the critical temperature T_c .

This question has been addressed in the context of the electroweak phase transition in the works listed in Ref. [14]. The common assumption of these works is that for weak enough transitions the dynamics is dominated by correlation-volume large-amplitude thermal fluctuations, dubbed subcritical bubbles, which promote considerable phase mixing as the Universe cools below the critical temperature. Within the validity of this analytical approach it was shown that homogeneous nucleation is only justified for Higgs masses below 70 GeV or so, which is both dangerously close to the present lower bound on the Higgs mass [15], and to the limit of validity of the perturbatively evaluated effective potential [16]. Furthermore, as with any analytical treatment of nonequilibrium dynamics, many aspects of the complicated kinetics of the system are not included. For example, even though correlation-volume bubbles may be the dominant fluctuations about equilibrium, there will be bubbles of different sizes present which may percolate and also acquire some thermal velocity due to diffusive processes. It is clear that a final answer to the problem can only be given by a combination of analytic and numerical tools.

In order to clarify the distinction between ‘weak’ and ‘strong’ first order transitions, one of us has recently studied the nonequilibrium dynamics of a (2+1)-dimensional model of a scalar field coupled to a thermal bath [17]. The nonlinear interactions were chosen to reflect the gross properties of the electroweak effective potential, although the model only deals with a real scalar field. It was shown that there is a very clear distinction between a weak and a strong transition, and that one should expect a very different dynamics between the two cases. In the present work, we generalize these results to (3+1)-

dimensions and also address important issues concerning the reliability of the numerical results. As we will show, it is clear that the two regimes are easily distinguishable, as in the (2+1)-dimensional case. Using homogeneous nucleation can easily lead to the wrong description of the dynamics.

In passing, we note that somewhat similar results have been obtained in the context of binary-fluid mixtures, where the (conserved) order parameter is the local concentration of one of the components of the mixture [18]. If the system is quenched to concentrations above the spinodal (the inflection point in the free-energy density), the transition evolves by spinodal decomposition; otherwise, nucleation occurs. The transition between the two regimes was shown in that case to be smooth. However, we must remember that here we are dealing with a non-conserved order parameter and have much faster dynamics than in binary fluid mixtures. As we will show, the transition between the two regimes is more dramatic in our context.

This paper is organized as follows. In the next Section we introduce the model we will use in the numerical simulations. In Section 3 we discuss details of the numerical approach used to study the dynamics of the system, including the implementation of the code on a parallel machine. In Section 4 we discuss the numerical results and their reliability. We conclude in Section 5 with a summary of our results and an outlook into future work.

II. THE MODEL

The homogeneous part of the free energy density is written as

$$U(\phi, T) = \frac{a}{2} (T^2 - T_2^2) \phi^2 - \frac{\alpha}{3} T \phi^3 + \frac{\lambda}{4} \phi^4 . \quad (5)$$

This choice intentionally resembles the electroweak effective potential to some order in perturbation theory, although here $\phi(\mathbf{x}, t)$ is a real scalar field, as opposed to the magni-

tude of the Higgs field. The goal is to explore the possible dynamics of a model described by the above free-energy density, generalizing the results obtained in Ref. [17] to (3+1)-dimensions. The analogy with the electroweak model is suggestive but not quantitative.

Introducing dimensionless variables $\tilde{x} = a^{\frac{1}{2}}T_2x$, $\tilde{t} = a^{\frac{1}{2}}T_2t$, $X = a^{-\frac{1}{4}}T_2^{-1}\phi$, and $\theta = T/T_2$, the Hamiltonian is,

$$\frac{H[X]}{\theta} = \frac{1}{\theta} \int d^2\tilde{x} \left[\frac{1}{2} |\tilde{\nabla}X|^2 + \frac{1}{2} (\theta^2 - 1) X^2 - \frac{\tilde{\alpha}}{3} \theta X^3 + \frac{\tilde{\lambda}}{4} X^4 \right], \quad (6)$$

where $\tilde{\alpha} = a^{-\frac{3}{4}}\alpha$, and $\tilde{\lambda} = a^{-\frac{1}{2}}\lambda$ (henceforth we drop the tildes). For temperatures above $\theta_1 = (1 - \alpha^2/4\lambda)^{-\frac{1}{2}}$ there is only one minimum at $X = 0$. At $\theta = \theta_1$ an inflection point appears at $X_{\text{inf}} = \alpha\theta_1/2\lambda$. Below θ_1 the inflection point separates into a maximum and a minimum given by $X_{\pm} = \frac{\alpha\theta}{2\lambda} \left[1 \pm \sqrt{1 - 4\lambda(1 - 1/\theta^2)/\alpha^2} \right]$. At the critical temperature $\theta_c = (1 - 2\alpha^2/9\lambda)^{-\frac{1}{2}}$ the two minima, at $X_o = 0$ and X_+ are degenerate. Below θ_c the minimum at X_+ becomes the global minimum and the X_o -phase becomes metastable. Finally, at $\theta = 1$ the barrier between the two phases at X_- disappears.

The coupling with the thermal bath will be modelled by a Markovian Langevin equation which, in terms of the dimensionless variables defined above, is

$$\frac{\partial^2 X}{\partial t^2} = \nabla^2 X - \eta \frac{\partial X}{\partial t} - \frac{\partial U(X, \theta)}{\partial X} + \xi(x, t), \quad (7)$$

where η is the dimensionless viscosity coefficient, and ξ the dimensionless stochastic noise with vanishing mean, related to η by the fluctuation-dissipation theorem,

$$\langle \xi(\mathbf{x}, t) \xi(\mathbf{x}', t') \rangle = 2\eta\theta\delta(t - t')\delta^3(\mathbf{x} - \mathbf{x}') . \quad (8)$$

A few comments are in order concerning our choice of equation. It is clear that we are assuming that $X(\mathbf{x}, t)$ represents the long-wavelength modes of the scalar field. Whenever one discretizes a continuum system there is an implicit coarse-graining scale built in. We encapsulate information about the shorter-wavelength modes, which have faster

relaxation time-scales, in the dissipation and noise terms. In principle it should be possible to derive an effective Langevin-like equation for the slow modes by integrating out the fast modes from the effective action. This is a complicated problem, and progress has been slow. Recent work indicates that one should expect departures from the Langevin equation written above [19], although details are sensitive to the particular model one starts with. For example, the noise may be colored (with more complicated correlation functions) and the coupling to the bath may be multiplicative, as opposed to the additive coupling chosen above. Here, we will adopt the above equation as a first step. We do not expect that the nature of the noise will change the final equilibrium properties of the system, but mostly the relevant relaxation time-scales. Since the physical results here are related to the final equilibrium state of the system, we believe that they will not be affected by more complicated representations of the coupling of the field to the thermal bath. However, a more thorough examination of this question deserves further study.

A related topic is the choice of coarse-graining scale, which is embedded in the lattice spacing used in the simulations. It is well-known that any classical field theory in more than one spatial dimension is ultra-violet divergent, and that the lattice spacing serves as an ultra-violet cutoff. This being the case, one should be careful when mapping from the lattice to the continuum theory. If one is to probe physics at shorter wavelengths, renormalization counterterms should be included in the lattice formulation so that a proper continuum limit is obtained on the lattice within the validity of perturbation theory. This point has been emphasized in Ref. [20], where a (2+1)-dimensional study of nucleation was performed for a temperature-independent potential. Renormalization counterterms (of order $\theta \ln \delta x$ for lattice spacing δx) for a particular renormalization prescription were obtained, and the results shown to be lattice-space independent.

Here, due to the temperature dependence of the potential, the renormalization prescription of Ref. [20] does not work. Instead, we will use $\delta x = 1$ throughout this work.

It turns out that for all cases studied the mean-field correlation length $\xi^{-2} = V''(X_o, \theta_c)$ is sufficiently larger than unity to justify this choice. Modes with shorter wavelengths are coupled through the noise into the dynamics of the longer wavelength modes, as described by equation 7 above.

III. LATTICE FORMULATION

The system is now discretized onto a lattice of length L with grid spacing δx , time step δt , and total run time Δt . Using a standard second order staggered leapfrog approach equation 7 becomes

$$\begin{aligned} \dot{X}_{i,n+1/2} &= \frac{1}{1 + \frac{1}{2}\eta t_n} \left[\left(1 - \frac{1}{2}\eta t_n\right) \dot{X}_{i,n-1/2} + \delta t \left(\nabla^2 X_{i,n} - \left. \frac{\partial U}{\partial X} \right|_{i,n} + \xi_{i,n} \right) \right] \\ X_{i,n+1} &= X_{i,n} + \delta t \dot{X}_{i,n+1/2} \end{aligned} \quad (9)$$

where i -indices are spatial and n -indices temporal. The continuum white noise $\xi(\mathbf{x}, t)$ is replaced by its discretized analogue $\xi_{i,n}$ by requiring that the discrete noise be uncorrelated on all scales above the shortest simulated. The discretised form of the fluctuation-dissipation relation of equation 8 becomes

$$\langle \xi_{i_1, n_1} \xi_{i_2, n_2} \rangle = 2\eta\theta \frac{1}{\delta t} \delta_{n_1, n_2} \frac{1}{(\delta x)^3} \delta_{i_1, i_2} \quad . \quad (10)$$

The discrete noise is hence approximated by

$$\xi_{i,n} = \sqrt{\frac{2\eta\theta}{\delta t (\delta x)^3}} \mathcal{G}_{i,n} \quad (11)$$

where $\mathcal{G}_{i,n}$ is a unit-variance Gaussian random number at each point in lattice spacetime.

Since we are modelling an unbounded system we do not want our simulation volume to have a distinct surface; we therefore use periodic boundary conditions. However, such boundary conditions may induce errors if a simulation runs for longer than a time causally

equivalent to $L/2$ as the periodicity then introduces spurious long-range correlations. Since we must run very long simulations to guarantee equilibration, were this constraint to apply we would be forced to use impossibly large lattices. Fortunately, the presence of the noise term, uncorrelated at each point in lattice spacetime, has the effect of swamping any such effect.

We must now run our simulations on large lattices (to reduce finite size effects) many times over (to reduce statistical noise) and for long run times (to ensure reaching equilibrium). Typically any attempt to reduce one of these constraints is met by a corresponding increase in another — for example, smaller grids give noisier results requiring more runs. As a consequence, we soon find ourselves at the limits of what is possible on a workstation. We have therefore parallelised the code and implemented it on a 128-node AP1000. The overall lattice is subdivided into an appropriate number of sub-lattices, each of which is local to a single node. These sub-lattices are defined with an overlap, such that each edge of any node's sub-lattice is included within the body of one of its neighbours. At each time step each node evolves the body of its local sub-lattice, but not the edges, for which insufficient data is locally available to calculate spatial derivatives. Each node then swaps the necessary data to update the overlapping edges of their associated sub-lattices with each of its neighbouring nodes.

The one qualitatively different feature of the parallel code is in the implementation of the random number generator. Computational random number generators are required to produce the same sequence of numbers whenever they are given the same initial conditions. Therefore what they actually generate, at least ideally, is a predictable, periodic, sequence of pseudo-random numbers, any sufficiently short (*i.e.* substantially shorter than the period) subset of which has statistical properties indistinguishable from a genuine random sequence. In our case we need random numbers at every point in lattice spacetime which are uncorrelated across the entire simulation spacetime; each node

requires numbers which are random not only locally at the node itself, but also across all the other nodes too. Either each node must have a different generator (highly impractical for any more than a few nodes) or each node must be allocated a unique subsequence of a single generator’s full sequence. Most generators are based on an iterative scheme, where each number in the sequence is calculated from some of the previous numbers in the sequence. However, if these previous numbers are not members of the local subsequence then there is a communication cost incurred in fetching them from the relevant node. In order to maximise the efficiency of the code, we require a generator whose sequence can be broken down into subsequences with elements generated by reference to previous members of that subsequence alone. Moreover, for large lattices and long run times we require a generator with an extremely long period. Thus for $L = 48$, $\delta t = 0.1$, and a running to $\Delta t = 3000$ (values used below) we require of the order of 2^{31} random numbers, and hence a generator with a period many times longer than this. A solution to this problem, applicable across any 2^n nodes, with a period of $2^{607} - 1$ and with each element in each subsequence calculable completely locally, is given by a particularly elegant parallelisation of the generalised feedback shift register algorithm [21]; this is the generator implemented here.

IV. NUMERICAL EXPERIMENT AND RESULTS

As pointed out in the Introduction, the question as to whether a first order phase transition is ‘weak’ or ‘strong’ boils down to how well localized in the metastable state the system is as the temperature drops below the critical temperature. In order to address this question, following the procedure of Ref. [17], we will study the behavior of the system at the critical temperature, when the two minima are degenerate. The reason for this choice follows naturally from the fact that we are interested on the way

by which the system approaches equilibrium as the temperature drops below T_c . The detailed dynamics will depend on the relative fraction of the total volume occupied by each phase; if at T_c the system is well localized about the $X = 0$ minimum, as the temperature drops the transition may evolve by nucleation and subsequent percolation of bubbles larger than a critical size. If, on the other hand, considerable phase-mixing occurs already at T_c , we expect the transition to evolve by domain coarsening, with the domains of the X_+ phase eventually permeating the whole volume.

Let us call the two phases the 0-phase and the +-phase, corresponding to the local equilibrium values $X = X_o = 0$, and $X = X_+$, respectively. We can quantify the phase distribution of the system as it evolves according to equation 7, by measuring the fraction of the total volume in each phase. This is done by simply counting the total volume of the system at the left of the potential barrier's maximum height (*i.e.*, $X \leq X_- \equiv X_{\max}$), corresponding to the 0-phase. Dividing by the total volume, we obtain the fraction of the system in the 0-phase, $f_o(t)$, such that

$$f_o(t) + f_+(t) = 1 \quad , \quad (12)$$

where, of course, $f_+(t)$ corresponds to the fractional volume in the +-phase.

A further measure of any configuration is given by the volume-averaged order parameter, $\langle X \rangle(t) = V^{-1} \int dV X(t)$. A localised configuration ($f_o^{\text{eq}} > 0.5$) then corresponds to $\langle X \rangle^{\text{eq}} < X_{\max}$, and a fully phase-mixed configuration ($f_o^{\text{eq}} \simeq 0.5$) to $\langle X \rangle^{\text{eq}} = X_{\max}$, where the superscript 'eq' refers to final ensemble-averaged equilibrium values of $f_o(t)$ and $\langle X \rangle(t)$.

We prepare the system so that initially it is well localised in the 0-phase, with $f_o(0) = 1$ and $\langle X \rangle(0) = 0$. These initial conditions are clearly the most natural choice for the problem at hand. If one has cosmology in mind, it is quite possible that as the system slowly cools down (we are not interested in phase transitions close to the Planck scale),

fluctuations from the high temperature phase $X = 0$ to the X_+ phase are already occurring before T_c is reached. (In this case, our arguments are even stronger.) However, we will adopt the best-case scenario for homogeneous nucleation to work, in which the system managed to reach the $X = 0$ phase homogeneously, so that the initial state is a thermal state with mean at X_0 . If one has more concrete applications in mind, we can assume that we quenched the system to its critical temperature, making sure that the order parameter remains localized about the high-temperature phase. Since thermalization happens very fast in the simulations, the exact point by point initial conditions should not be important, and we can view the first few time steps as generating an initial thermal distribution with $f_o(0) \sim 1$ and $\langle X \rangle \sim 0$, so that the average kinetic energy per lattice point satisfies the equipartition theorem, $\frac{1}{N}E_k = \frac{3}{2}T$. For simplicity we take $X = 0, \dot{X} = 0$ everywhere initially.

There are two parameters controlling the strength of the transition, α and λ . In the previous (2+1)-dimensional work, α was chosen to vary while λ was kept fixed. It is really immaterial which parameter is held fixed, or if both are made to vary, but in order to keep closer to the spirit of the electroweak model we will fix α and let λ vary. As is well-known, λ is related to the Higgs mass, while α is related to the gauge-boson masses [2]. The connection with the electroweak model is straightforward. If we consider as an example the unimproved one-loop approximation, the effective potential is [2],

$$V_{\text{EW}}(\phi, T) = D (T^2 - T_2^2) \phi^2 - ET\phi^3 + \frac{1}{4}\lambda_T\phi^4, \quad (13)$$

where D and E are given by $D = [6(M_W/\sigma)^2 + 3(M_Z/\sigma)^2 + 6(M_T/\sigma)^2]/24 \simeq 0.17$ and $E = [6(M_W/\sigma)^3 + 3(M_Z/\sigma)^3]/12\pi \simeq 0.097$, for $M_W = 80.6$ GeV, $M_Z = 91.2$ GeV, $M_T = 174$ GeV [22], and $\sigma = 246$ GeV. T_2 is given by,

$$T_2 = \sqrt{(M_H^2 - 8B\sigma^2)/4D}, \quad (14)$$

where the physical Higgs mass is given in terms of the 1-loop corrected λ as $M_H^2 =$

$(2\lambda + 12B) \sigma^2$, with $B = (6M_W^4 + 3M_Z^4 - 12M_T^4) / 64\pi^2 \sigma^4$, and the temperature-corrected Higgs self-coupling is,

$$\lambda_T = \lambda - \frac{1}{16\pi^2} \left[\sum_B g_B \left(\frac{M_B}{\sigma} \right)^4 \ln \left(M_B^2 / c_B T^2 \right) - \sum_F g_F \left(\frac{M_F}{\sigma} \right)^4 \ln \left(M_F^2 / c_F T^2 \right) \right] \quad (15)$$

where the sum is performed over bosons and fermions (in our case only the top quark) with their respective degrees of freedom $g_{B(F)}$, and $\ln c_B = 5.41$ and $\ln c_F = 2.64$.

Thus, the correspondence with our (dimensionless) parameters is

$$\alpha = \frac{3E}{(2D)^{\frac{3}{4}}} = 0.065, \quad \text{and} \quad \lambda = \frac{\lambda_T}{(2D)^{\frac{1}{2}}} = 1.72\lambda_T. \quad (16)$$

Once this is established, the numerical experiment proceeds as follows: i) Choose $\alpha = 0.065$; ii) Prepare the system in the initial state described above, and measure the value of $f_o(t)$ and $\langle X \rangle(t)$ for several values of λ , as the system evolves according to equation 7. As with any numerical experiment, one must make sure that the results are independent of lattice artifacts (or at least the dependence is understood), such as its finite size and choice of time-step for the evolution routine. Before we discuss our results, we will address these issues in the following Subsection.

A. Finite Lattices and the Thermodynamic Limit

Whenever simulating a system on the lattice, we are faced with the hard decision of having to achieve a compromise between approximating the infinite volume limit, and having fairly reasonable integration times. This problem is particularly serious in the context of phase transitions, as it is well-known that symmetry breaking only occurs in the infinite volume limit; at finite volumes, there is a nonzero probability that a large fluctuation will restore the broken symmetry. Even though this is formally true, we will argue here that this does not represent a problem to our simulations, if we make sure that the lattice is large enough. There is a large amount of literature on finite-size effects

and how they are handled in different contexts [23], and we do not intend to reproduce these results. What we want to do is to bring this issue closer to our problem.

We are interested in studying the system given by the free-energy density of equation 5, at the critical temperature θ_c when the two minima are degenerate. The system is prepared in the 0-phase, and we measure the fraction of the volume in each phase as it evolves. We will give a rough estimate of how large the lattice should be in order to suppress spurious symmetry restoration (that is, $f_o \rightarrow 0.5$, in our case) due to the lattice size. There are two relevant time-scales in the problem, the relaxation time-scale for small-amplitude fluctuations within the $X = 0$ well, τ_{rel} , and the ‘escape’ time-scales for large amplitude fluctuations into the +-phase, τ_{esc} . In terms of the rate per unit volume for each process, we write the relevant time-scales as

$$V\Gamma_{\text{rel}} \sim \tau_{\text{rel}}^{-1} \sim T\gamma_{\text{rel}}^{-1} \quad , \quad (17)$$

where γ_{rel} is the typical relaxation time-scale for short amplitude fluctuations in units of T^{-1} , and

$$V\Gamma_{\text{esc}} \sim \tau_{\text{esc}}^{-1} \sim T\exp[-F_f/T] \quad , \quad (18)$$

where F_f is the free energy of the large amplitude fluctuation. The condition for large amplitude fluctuations to be suppressed in comparison to typical relaxation processes is then,

$$\frac{\tau_{\text{esc}}}{\tau_{\text{rel}}} \gg 1 \quad \Rightarrow \quad \exp[F_f/T] \gg \gamma_{\text{rel}} \quad . \quad (19)$$

To estimate τ_{esc} note that within the Gaussian approximation, a homogeneous fluctuation of volume V and amplitude ϕ_A about equilibrium ($\phi = 0$, for simplicity) has free energy

$$F_f(\phi_A, V, T) = \frac{V}{2}m^2(T)\phi_A^2 \quad , \quad (20)$$

where $m^2(T) = V''(\phi = 0, T)$ (we neglect the gradient contribution, as it would suppress the fluctuation even further, making our arguments stronger). We are interested in fluctuations about $X = 0$ (we now go back to our dimensionless variables), at the critical temperature $\theta_c = (1 - 2\alpha^2/9\lambda)^{-\frac{1}{2}}$. We expect growing instabilities to be triggered whenever fluctuations probe the nonlinearities in the free energy. This is corroborated by the results in Ref. [17] and, as we will soon see, here also. Thus we consider fluctuations with amplitude equal to the nearest inflection point to $X = 0$, namely $X_A = \frac{\alpha\theta_c}{3\lambda} (1 - 1/\sqrt{3})$. Writing their volume $V = \frac{4\pi}{3} (n\xi)^3$ in terms of the correlation length $\xi(\theta_c) = (\theta_c^2 - 1)^{-\frac{1}{2}}$, with n a real number, we obtain

$$\frac{F_f}{\theta_c} \simeq 0.088 \frac{\alpha}{\lambda^{3/2}} n^3 \quad . \quad (21)$$

From our arguments above it is clear that $\gamma_{\text{rel}} = (\theta_c^2 - 1)^{-\frac{1}{2}}$. Let us consider an example which will be relevant later on. Take $\alpha = 0.065$ and $\lambda = 0.020$. In this case, the correlation length is $\xi(\theta_c) \simeq 4.5$ and we obtain, from equation 19, $n \gg 0.91$. Since the radius of the fluctuation is $R_f = n\xi$ this result implies that fluctuations probing the inflection point with radius $R_f = 0.91 \times 4.5 \simeq 4.1$ are probable within typical relaxation time scales of the system. Thus the lattice length L should be sufficiently larger than about $2R_f$ ($L \geq 10$ or so) to avoid spurious symmetry restoration. For $L = 20$ the volume ratio of the lattice to the above fluctuations is around $L^3/4R_f^3 \sim 25$, and such processes alone cannot restore the symmetry within time-scales of interest in the dynamics. In all the results quoted in this work we use $L = 48$.

We give two pieces of evidence supporting these arguments. In Fig.1 the equilibrium values of the 0-phase fraction, f_o^{eq} , and of the volume-averaged order parameter, $\langle X \rangle^{\text{eq}}$, are given as a function of the lattice size L , for $\alpha = 0.065$ and $\lambda = 0.020$. λ is chosen so that for large lattices the system remains localized mostly in the 0-phase. Note that as L decreases $f_o^{\text{eq}} \rightarrow 0.5$, representing a spurious ‘symmetry restoration’ due to the smallness

of the lattice. For small lattices, the two phases are completely mixed. In fact, changes can be seen between $L = 10$ and $L = 20$, in qualitative agreement with our arguments above. Note that for large enough lattices, the equilibrium value approaches a stable value which is independent of the lattice size. For all practical purposes, this is the infinite volume limit. Fluctuations large enough to restore the symmetry are possible, but with negligible probability.

The reader may wonder why for large enough lattices $f_o^{\text{eq}} \neq 1$. The reason for this is that at finite temperatures there is a nonvanishing probability per unit volume of having thermal fluctuations populating the $+-$ phase. Even though these fluctuations are unstable and shrink away, there will be an equilibrium distribution of bubbles suppressed by a Boltzmann factor. For very strong transitions (very small λ), $f_o^{\text{eq}} \sim 1$, and a negligible fraction of the system is in the $+-$ phase. We refer the reader to the paper by Gelmini and Gleiser, Ref. [14] for details. In Fig. 2 we show a phase space portrait of the system for a given point on the lattice for different lattice sizes. That is, we choose a particular point $X(x_o, y_o, z_o, t)$ and follow its evolution, making a plot of $\dot{X}(x_o, y_o, z_o, t)$ vs $X(x_o, y_o, z_o, t)$. Taking $\alpha = 0.065$ and $\lambda = 0.010$, Fig. 2a shows the $L = 4$ and Fig. 2b the $L = 20$ case. It is clear that for the smaller lattice the system is probing both minima of the free energy ($X_o = 0$ and $X_+ = 4.55$ here), while for the larger lattice the system remains localized in the $X = X_o$ well. As the lattice size is increased the throat separating the two minima becomes less and less dense until eventually the system becomes ‘trapped’ within one well. The time-scale for its eventual escape is much larger than any time-scale of interest in this problem, with $\tau_{\text{esc}} \rightarrow \infty$ as $L \rightarrow \infty$.

Finally, in Fig. 3, we show the equilibrium values of the fraction $f_o(t)$, f_o^{eq} , and of the volume-averaged order parameter, $\langle X \rangle^{\text{eq}}$, for $\alpha = 0.065$ and $\lambda = 0.020$, as a function of time step, δt . Note that using too large a time step compromises the stability of the simulations, tending to drive the system’s equilibrium towards the phase-mixed

symmetric state ($f_o^{\text{eq}} \rightarrow 0.5$, $\langle X \rangle^{\text{eq}} = X_{\text{max}}$). The results detailed below are therefore obtained using a time step $\delta t = 0.1$.

B. Numerical Results

Based on the above discussion, we choose $L = 48$, $\delta x = 1$, $\delta t = 0.1$, and $\alpha = 0.065$ in all simulations. The experiment then consists in measuring the fraction of the volume in the 0-phase as a function of time for several values of λ . As this involves a stochastic noise, we must perform an ensemble average over many runs in order to obtain physically reasonable results.

In Fig. 4 we show the evolution of the ensemble-averaged fraction $f_o(t)$ for several values of λ . It is clear that for small enough values of λ the system remains well-localized in the 0-phase with $f_o^{\text{eq}} \sim 1$, while for larger values the two phases become completely mixed, with $f_o^{\text{eq}} \rightarrow 0.5$. Remarkably, the transition region between the two regimes is quite narrow, centered around $\lambda \simeq 0.025$. This can be seen from Fig. 5 where we show $f_o(t)$ for $\lambda = 0.024$, 0.025 , and 0.026 . [The curves are noisier due to the fact that we must run for longer times in order to approach the equilibrium values of $f_o(t)$, being thus constrained to perform an ensemble average with fewer runs.] Note that for $\lambda = 0.026$, $f_o^{\text{eq}} \simeq 0.5$, while for $\lambda = 0.024$, $f_o^{\text{eq}} \simeq 0.72$. There is a pronounced change in the behavior of the system for $\lambda \simeq 0.025$. Furthermore, we find that the numerical curves can be fitted at all times by a stretched exponential,

$$f_o(t) = (1 - f_o^{\text{eq}}) \exp[-(t/\tau_{\text{eq}})^\sigma] + f_o^{\text{eq}} \quad , \quad (22)$$

where f_o^{eq} is the final equilibrium fraction and τ_{eq} is the equilibration time-scale. In Table 1 we list σ and τ_{eq} for several values of λ . Note that for $\lambda = 0.025$ the fit is obtained at late times by a power law, (smooth dashed curve in Fig. 5)

$$f_o(t) |_{\lambda=0.025} \propto t^{-k} , \quad (23)$$

with $k = 0.10(\pm 0.02)$. This slowing down of the approach to equilibrium is typical of systems in the neighborhood of a second order phase transition, being known as ‘critical slowing down’ [24]. This behavior is suggestive of a phase transition between two possible regimes for the system, one in which the system is well-localized in the 0-phase, and the other in which there is a complete mixing between the two phases. Let us call these two regimes the ‘strong’ and the ‘weak’ regimes, respectively. Before we explore this idea any further, it is prudent to check if the final equilibrium fractions are sensitive to the viscosity parameter η , which reflects the coupling of the system to the thermal bath. In Fig. 6 we show the approach to equilibrium for several values of η and for $\lambda = 0.020$, which lies within the ‘strong’ regime. It is clear that whereas the equilibration time-scales are sensitive to the value of η , with larger η implying slower equilibration, the *final* equilibrium fractions are the same. This is precisely what one expects, as the coupling to the bath should not influence the final equilibrium properties of the system, but only how fast it equilibrates.

Armed with these results, and invoking also the results in $(2+1)$ -dimensions [17], we define the equilibrium fractional population difference

$$\Delta F^{\text{eq}}(\theta_c) = f_o^{\text{eq}} - f_+^{\text{eq}} . \quad (24)$$

In Fig. 7 we show the behavior of ΔF^{eq} as a function of λ . There is a clear qualitative analogy between the behavior of ΔF^{eq} as a function of λ and the behavior of the magnetization as a function of temperature in Ising models. Here, the order parameter is the equilibrium fractional population difference and the control parameter is λ . $\lambda_c \simeq 0.025$ is the critical value for the parameter λ , which determines the degree of mixing of the system at T_c .

We stress that the idea here is to probe the assumption of localization within the

0-phase as the system cools to T_c . Our results show that if the time-scales for cooling are slower than the equilibration time-scales of the system, for $\lambda > \lambda_c$ there will be considerable phase mixing before the temperature drops below T_c . This result can be made quite transparent by comparing the equilibrium value of the volume-averaged field $\langle X \rangle^{\text{eq}}$, and the location of both the inflection point and the maximum of the potential with varying λ . As can be seen from Fig. 8, the narrow transition region is clearly delimited by

$$X_{\text{inf}} < \langle X \rangle^{\text{eq}} < X_{\text{max}} \quad , \quad (25)$$

where X_{inf} and X_{max} are the inflection point and the maximum of the potential barrier, respectively. Note that for $\lambda \geq 0.026$, $f_o^{\text{eq}} = 0.5$ and $\langle X \rangle^{\text{eq}} = X_{\text{max}}$. Recalling the information from Fig. 7, we conclude that there is a clear distinction between the ‘strong’ and ‘weak’ regimes. The existence of a potential barrier between the two phases at T_c does not imply in the system being localized in the 0-phase, for large enough values of λ . This efficient thermal mixing of the phases will affect the dynamics of the phase transition as the temperature drops below T_c . For $\lambda > 0.025$, if the cooling is slow enough, there is no reason to expect that the system will approach its final equilibrium by nucleation of bubbles larger than critical. Rather, the mechanism will resemble spinodal decomposition, where domains of the two phases will compete for dominance, with the +-phase eventually dominating the volume. We stress that the value $\lambda_c = 0.025$ is a weak lower bound; even if the system starts localized in the 0-phase at T_c for a smaller value of λ , the potential barrier will also decrease for lower temperatures, and we should expect departures from nucleation settling in even for $\lambda < 0.025$. [Of course, the decrease in temperature will also suppress thermal fluctuations.] The evaluation of the exact value of λ for which nucleation theory will break down depends on the asymmetry of the potential, the temperature, and on the cooling rate, requiring further study. However, we can assert

that this value will be at least lower than λ_c .

V. CONCLUSIONS AND OUTLOOK

In this paper we investigated the possibility that thermal fluctuations may induce considerable phase mixing for systems which exhibit two degenerate phases at their critical temperature. By modelling the nonequilibrium dynamics by means of a Langevin equation with the system initially localized in one phase, we showed that complete mixing of the two phases can occur, despite the presence of a potential barrier between the phases. These results are of importance in the context of cosmological phase transitions, in particular when the cooling rate is sufficiently slow compared to the equilibration time-scales of the system. This limit is implicit in our simulations, as we held the temperature fixed at T_c while the system equilibrated. Our results should also be of importance for systems studied in the laboratory. As we mentioned in the Introduction, binary fluid mixtures separate by spinodal decomposition if the system is initially quenched with concentrations above the spinodal. The dynamics in that case is much slower though, and the transition between nucleation and spinodal decomposition is smoother [18]. However, we believe the essential physics to be the same, as we found that considerable phase mixing occurred precisely as the equilibrium value of the volume-averaged scalar field (the equivalent of the concentration in the binary fluid case) traversed within the ‘transitional’ region delimited by the locations of the inflection point and the maximum of the potential barrier. Also, as mentioned in previous publications [14], this phase mixing is characteristic of pre-transitional phenomena found in the isotropic-nematic transition of liquid crystals, which is known to be ‘weakly’ first order [25].

Inspired by the effective potential of the electroweak model, we measured the degree of mixing with respect to the value of the quartic self-coupling of the scalar order parameter.

However, as mentioned before, this is not a simulation of the electroweak transition, as our order parameter is a real scalar field. In fact, the critical value above which we found that the two phases mix, $\lambda_c \simeq 0.025$, is below the value of λ which corresponds to a physical Higgs mass. Using the equivalence relation between the two models obtained in equation 16, a Higgs mass of $M_H = 50$ GeV would correspond to $\lambda = 0.0518$, which is well within the ‘weak’ regime. For this value of λ , the equilibrium value of the volume averaged field $\langle X \rangle^{\text{eq}} = X_{\text{max}}$, and the two phases are indistinguishable.

The results presented here are in qualitative agreement with a previous work in which phase mixing was investigated in (2+1)-dimensions [17]. As in that case, we suggest that the distinction between ‘weak’ and ‘strong’ first order transitions be quantified in terms of the equilibrium fractional population difference between the two phases, $\Delta F^{\text{eq}} = f_o^{\text{eq}} - f_+^{\text{eq}}$. Within the limits of a finite lattice, we observed a sharp change in the behavior of ΔF^{eq} with respect to λ , (see Fig. 7) which we suggest characterizes a second order phase transition between the ‘symmetric’ (‘weak’) phase $\Delta F^{\text{eq}} = 0$ and the ‘broken-symmetric’ (‘strong’) phase $\Delta F^{\text{eq}} = 1$. In order to study the details of the transition, a more thorough analysis of finite-size effects in the determination of the critical value $\lambda_c \simeq 0.025$ and of the critical exponent β , obtained from the relation $\Delta F^{\text{eq}} = (\lambda_c - \lambda)^\beta$ in the neighborhood of λ_c , must be performed. But taken together, the sharp change in ΔF^{eq} and the presence of critical slowing down about λ_c provide substantial evidence for the existence of this transition.

Finally, our work also calls for a more detailed analysis of the rôle of noise with spatio-temporal memory in simulations of the dynamics of phase transitions in field theories. The Markovian Langevin equation used here is certainly an approximation to more complicated couplings between the system and the thermal bath. It remains to be seen what rôle will colored noise play in the nonequilibrium dynamics of field theories. It is however hard to imagine that the nature of the noise can affect final equilibrium properties

of the system, although it may affect the equilibration time-scales. In this connection, we note that recent results by one of us show that at high enough temperatures, colored noise becomes white [19]. Given our present level of understanding of the nonequilibrium dynamics of field theories it is only fair to expect many surprises in the coming years.

ACKNOWLEDGMENTS

JB acknowledges the support and assistance of the Imperial College / Fujitsu Parallel Computing Research Center. MG was supported in part by a National Science Foundation Presidential Faculty Fellows Award No. PHY-9453431 and by grant No. PHYS-9204726. This collaboration was made possible by NATO Collaborative Research Grant ‘Cosmological Phase Transitions’ no. SA-5-2-05 (CRG 930904) 1082/93/JARC-501.

REFERENCES

- [1] For a review see E. W. Kolb and M. S. Turner, *The Early Universe*, (Addison-Wesley, Redwood, CA, 1990).
- [2] A. G. Cohen, D. B. Kaplan, and A. E. Nelson, *Annu. Rev. Nucl. Part. Sci.* **43**, 27 (1993); A. Dolgov, *Phys. Rep.* **222**, 311 (1992).
- [3] See, however, G. R. Farrar and M. E. Shaposhnikov, *Phys. Rev. Lett.* **70**, 2833 (1993); CERN preprint TH-6734/93, in press *Phys. Rev.* **D**.
- [4] B. Liu, L. McLerran, and N. Turok, *Phys. Rev.* **D46**, 2668 (1992); A. G. Cohen, D. B. Kaplan, and A. E. Nelson, *Phys. Lett.* **B336**, 41 (1994); M. B. Gavela, P. Hernández, J. Orloff, and O. Pène, *Mod. Phys. Lett.* **A9**, 795 (1994); P. Huet and E. Sather, preprint SLAC-PUB-6479 (1994); G. R. Farrar and M. E. Shaposhnikov, preprint Rutgers University RU-94-40.
- [5] R. Becker and W. Döring, *Ann. Phys.* **24**, 719 (1935).
- [6] J. W. Cahn and J. E. Hilliard, *J. Chem. Phys.* **31**, 688 (1959).
- [7] J. S. Langer, *Ann. Phys. (NY)* **41**, 108 (1967); *ibid.* **54**, 258 (1969).
- [8] J. D. Gunton, M. San Miguel and P. S. Sahni, in *Phase Transitions and Critical Phenomena*, **Vol. 8**, Ed. C. Domb and J. L. Lebowitz (Academic Press, London, 1983).
- [9] M. B. Voloshin, I. Yu. Kobzarev, and L. B. Okun', *Yad. Fiz.* **20**, 1229 (1974) [Sov. J. Nucl. Phys. **20**, 644 (1975)].
- [10] S. Coleman, *Phys. Rev.* **D15**, 2929 (1977); C. Callan and S. Coleman, *Phys. Rev.* **D16**, 1762 (1977).
- [11] A. D. Linde, *Phys. Lett.* **70B**, 306 (1977); *Nucl. Phys.* **B216**, 421 (1983); [Erratum: **B223**, 544 (1983)].

- [12] M. Gleiser, G. Marques, and R. Ramos, *Phys. Rev.* **D48**, 1571 (1993); D. E. Brahm and C. Lee, *Phys. Rev.* **D49**, 4094 (1994); D. Boyanovsky, D. E. Brahm, R. Holman, and D.-S. Lee, Carnegie Mellon University preprint No. CMU-HEP94-20.
- [13] P. Arnold and L. McLerran, *Phys. Rev.* **D36**, 581 (1987); *ibid.* **D37**, 1020 (1988).
- [14] M. Gleiser and E. W. Kolb, *Phys. Rev. Lett.* **69**, 1304 (1992); M. Gleiser and R. O. Ramos, *Phys. Lett.* **B300**, 271, (1993); G. Gelmini and M. Gleiser, *Nucl. Phys.* **B419**, 129 (1994); M. Gleiser, E. W. Kolb, and R. Watkins, *Nucl. Phys.* **B364**, 411 (1991).
- [15] Particle Data Group, *Phys. Rev.* **D50**, 1173 (1994).
- [16] W. Buchmüller and Z. Fodor, *Phys. Lett.* **B331**, 124 (1994); M. Gleiser and R. Ramos, Ref. [14].
- [17] M. Gleiser, Dartmouth preprint No. DART-HEP-94/01.
- [18] J. Langer, *Physica* **73**, 61 (1974); J. Langer, M. Bar-on, and H. Miller, *Phys. Rev.* **A11**, 1417 (1975).
- [19] M. Gleiser and R. Ramos, *Phys. Rev.* **D50**, 2441 (1994); B. L. Hu, J. P. Paz and Y. Zhang, in *The Origin of Structure in the Universe*, Ed. E. Gunzig and P. Nardone (Kluwer Acad. Publ. 1993); D. Lee and D. Boyanovsky, *Nucl. Phys.* **B406**, 631 (1993); S. Habib, in *Stochastic Processes in Astrophysics*, Proc. Eighth Annual Workshop in Nonlinear Astronomy (1993).
- [20] M. Alford and M. Gleiser, *Phys. Rev.* **D48**, 2838 (1993).
- [21] S. Aluru, G. M. Prabhu, and J. Gustafson, *Parallel Computing* **18**, 839 (1992).
- [22] F. Abe et al. (CDF Collaboration), *Phys. Rev. Lett.* **73**, 225 (1994); *ibid.*, *Phys. Rev.* **D50**, 2966 (1994).

- [23] *Finite Size Scaling and Numerical Simulations of Statistical Systems*, edited by V. Privman (World Scientific, Singapore, 1990).
- [24] *Statistical Field Theory*, C. Itzykson and J.-M. Drouffe, Cambridge Monographs on Mathematical Physics (Cambridge University Press, New York, 1989).
- [25] T. W. Stinson and J. D. Litster, *Phys. Rev. Lett.* **25**, 503 (1970); H. Zink and W. H. de Jeu, *Mol. Cryst. Liq. Cryst.* **124**, 287 (1985).

List of Figures

Figure 1. The equilibrium values of the 0-phase fraction f_o^{eq} and of the volume-averaged field $\langle X \rangle^{\text{eq}}$ are shown as a function of lattice length L for $\lambda = 0.020$.

Figure 2a. Phase space portrait for an arbitrarily chosen point of a lattice of length $L = 4$. $\lambda = 0.010$ in this run. Note how the system probes both minima of the potential.

Figure 2b. Phase space portrait for an arbitrarily chosen point of a lattice of length $L = 20$. $\lambda = 0.010$ in this run. Note how the system remains constrained within the 0-phase.

Figure 3. The equilibrium values of the 0-phase fraction f_o^{eq} and of the volume-averaged field $\langle X \rangle^{\text{eq}}$ are shown as a function of time step δt for $\lambda = 0.020$.

Figure 4. Evolution of the ensemble-averaged fraction $f_o(t)$ for several values of λ .

Figure 5. Evolution of the ensemble-averaged fraction $f_o(t)$ for a narrow range about the critical value $\lambda = 0.025$. The smooth dashed curve is the power law fit described in

equation 23.

Figure 6. Evolution of the ensemble-averaged fraction $f_o(t)$ for several values of the viscosity parameter η and for $\lambda = 0.020$. Note how the final equilibrium fraction is independent of the value of η .

Figure 7. The fractional equilibrium population difference ΔF^{eq} for several values of λ . Note the sharp discontinuity about the critical value $\lambda_c \simeq 0.025$.

Figure 8. Comparison of the equilibrium value of the volume-averaged field $\langle X \rangle^{\text{eq}}$ (circles), with the location of the nearest inflection point to $X = 0$, X_{inf} , and the potential barrier, X_{max} , as a function of λ . Note the existence of a transitional region for $0.021 \simeq \lambda < 0.026$. For $\lambda \geq 0.026$, $\langle X \rangle^{\text{eq}} = X_{\text{max}}$.

List of Tables

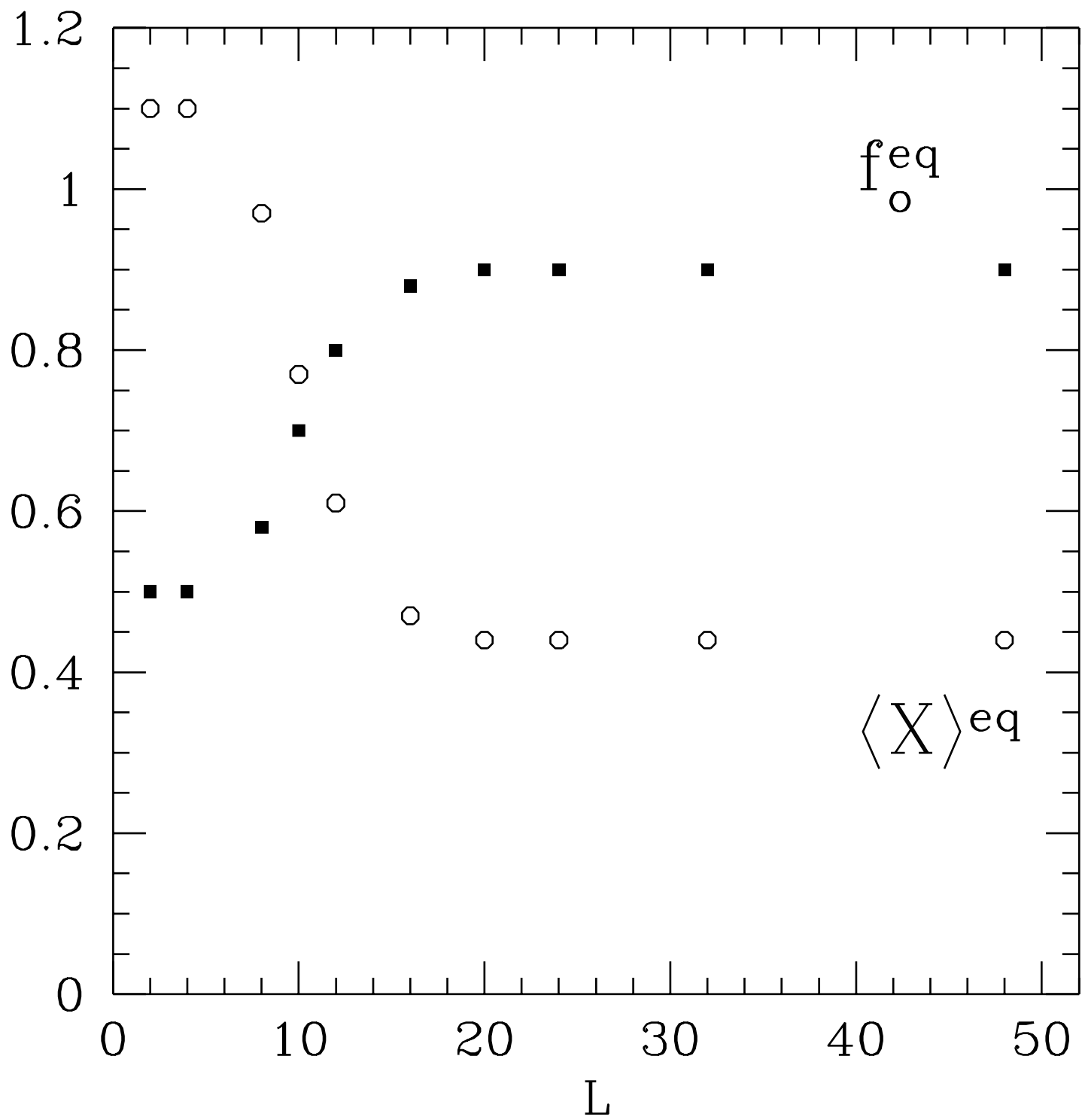
Table 1. The values of the equilibration time-scales and the exponents for the exponential fit of equation 22 for several values of λ .

TABLE 1

λ	τ_{EQ}	σ
0.015	25.0	1.0
0.020	45.0	1.0
0.022	60.0	1.0
0.024	110.0	0.80
0.026	220.0	0.50
0.028	120.0	0.75
0.030	100.0	0.80
0.035	55.0	0.80
0.040	40.0	0.90

This figure "fig1-1.png" is available in "png" format from:

<http://arxiv.org/ps/hep-ph/9410235v2>



This figure "fig2-1.png" is available in "png" format from:

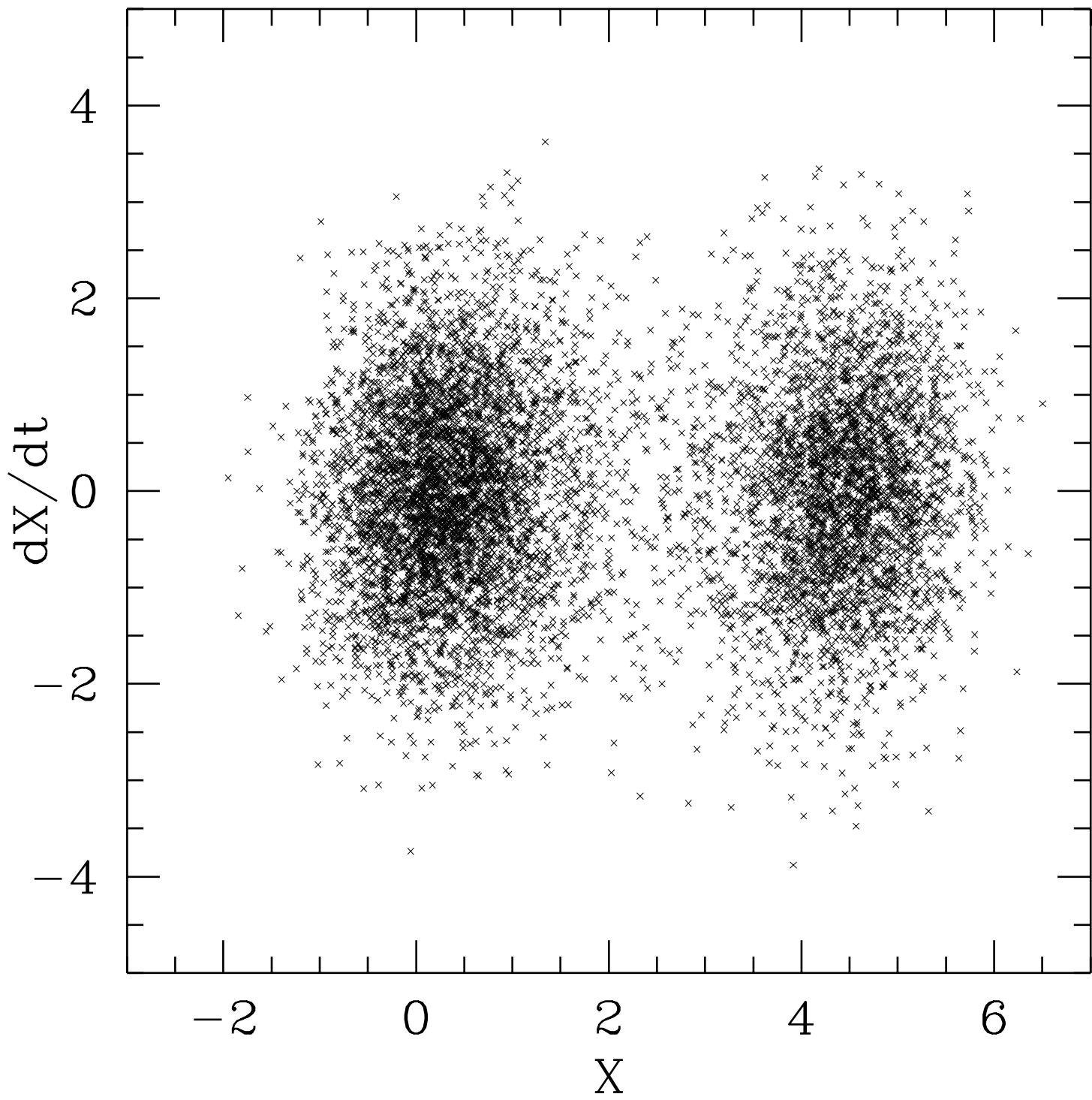
<http://arxiv.org/ps/hep-ph/9410235v2>

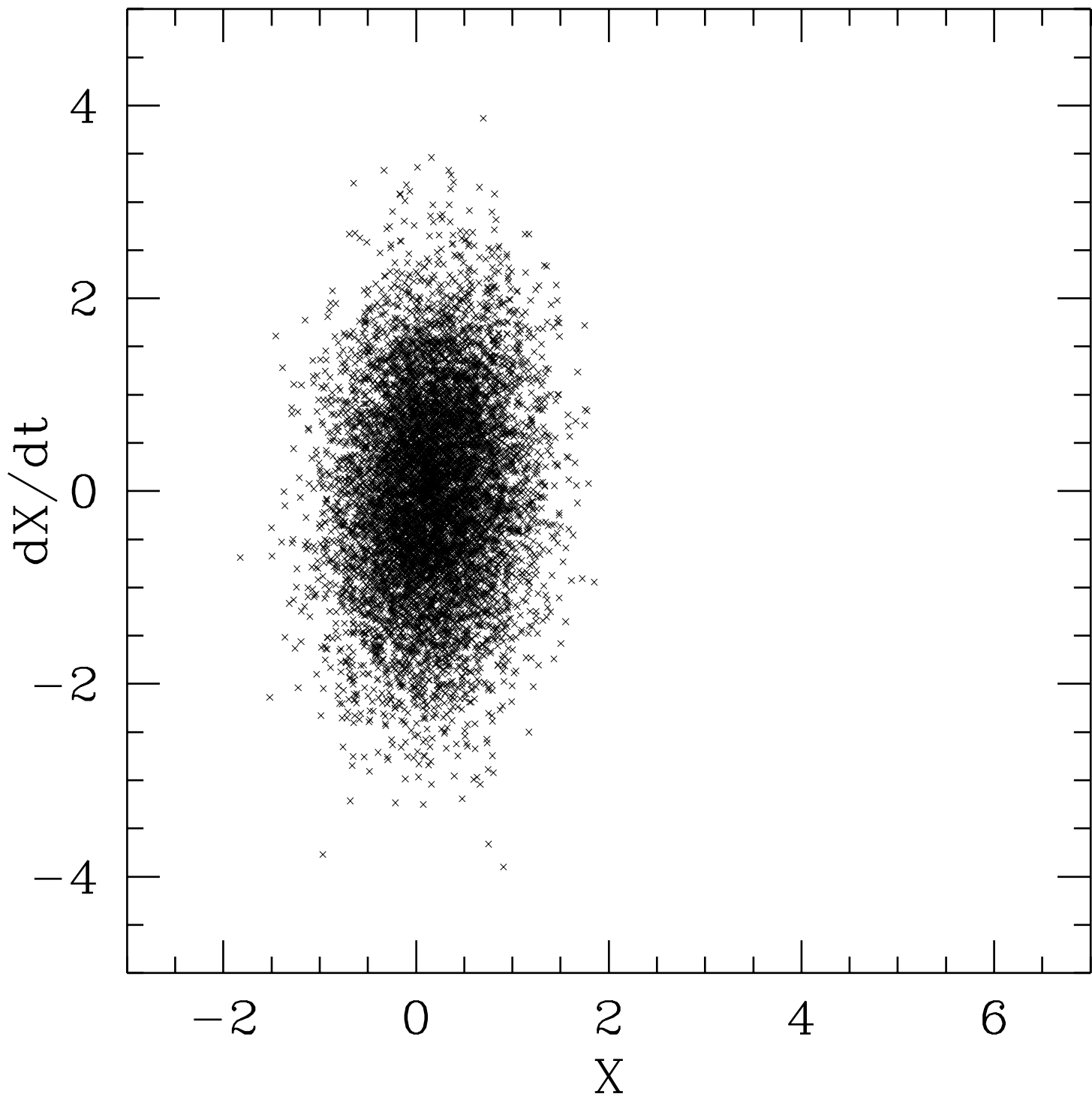
This figure "fig1-2.png" is available in "png" format from:

<http://arxiv.org/ps/hep-ph/9410235v2>

This figure "fig2-2.png" is available in "png" format from:

<http://arxiv.org/ps/hep-ph/9410235v2>



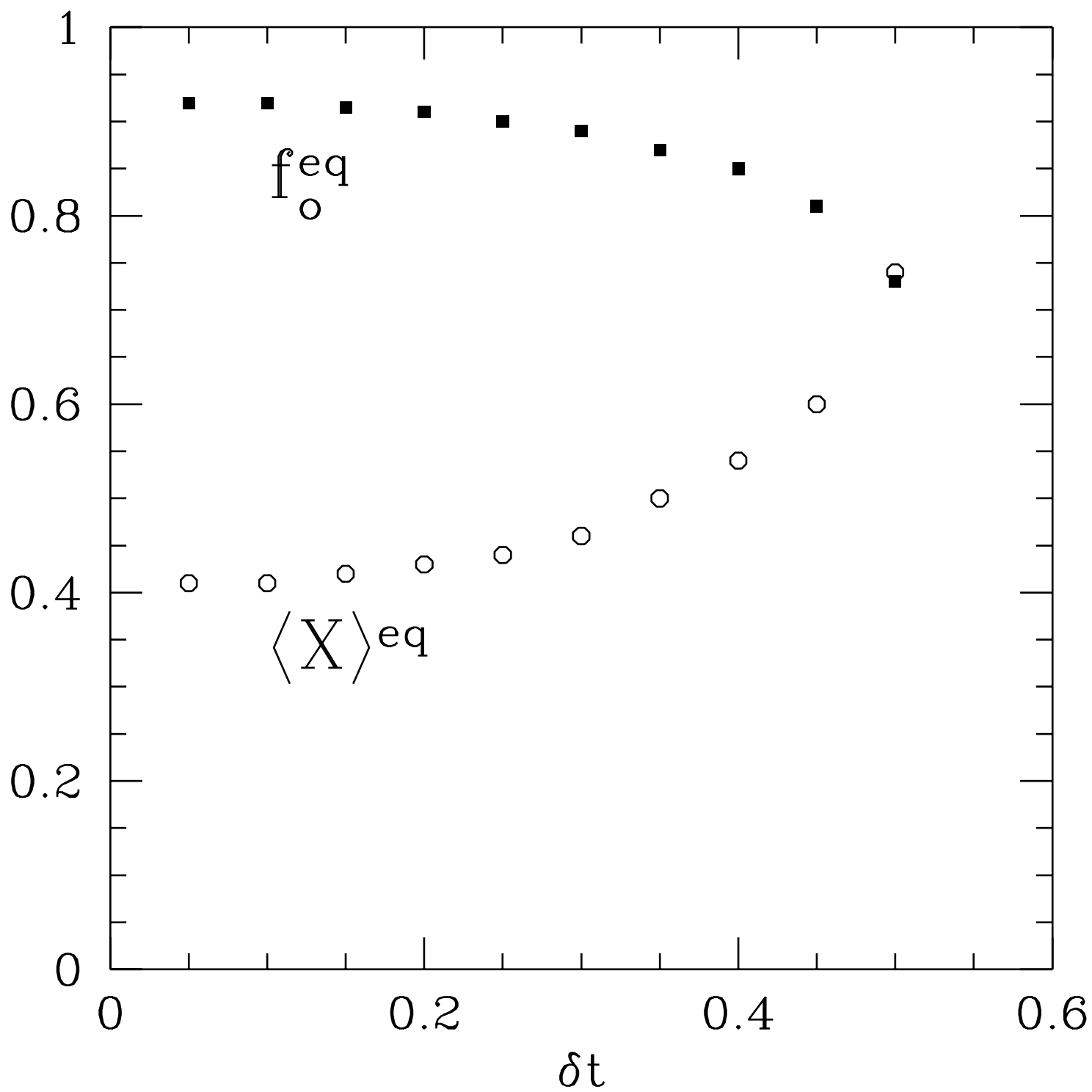


This figure "fig1-3.png" is available in "png" format from:

<http://arxiv.org/ps/hep-ph/9410235v2>

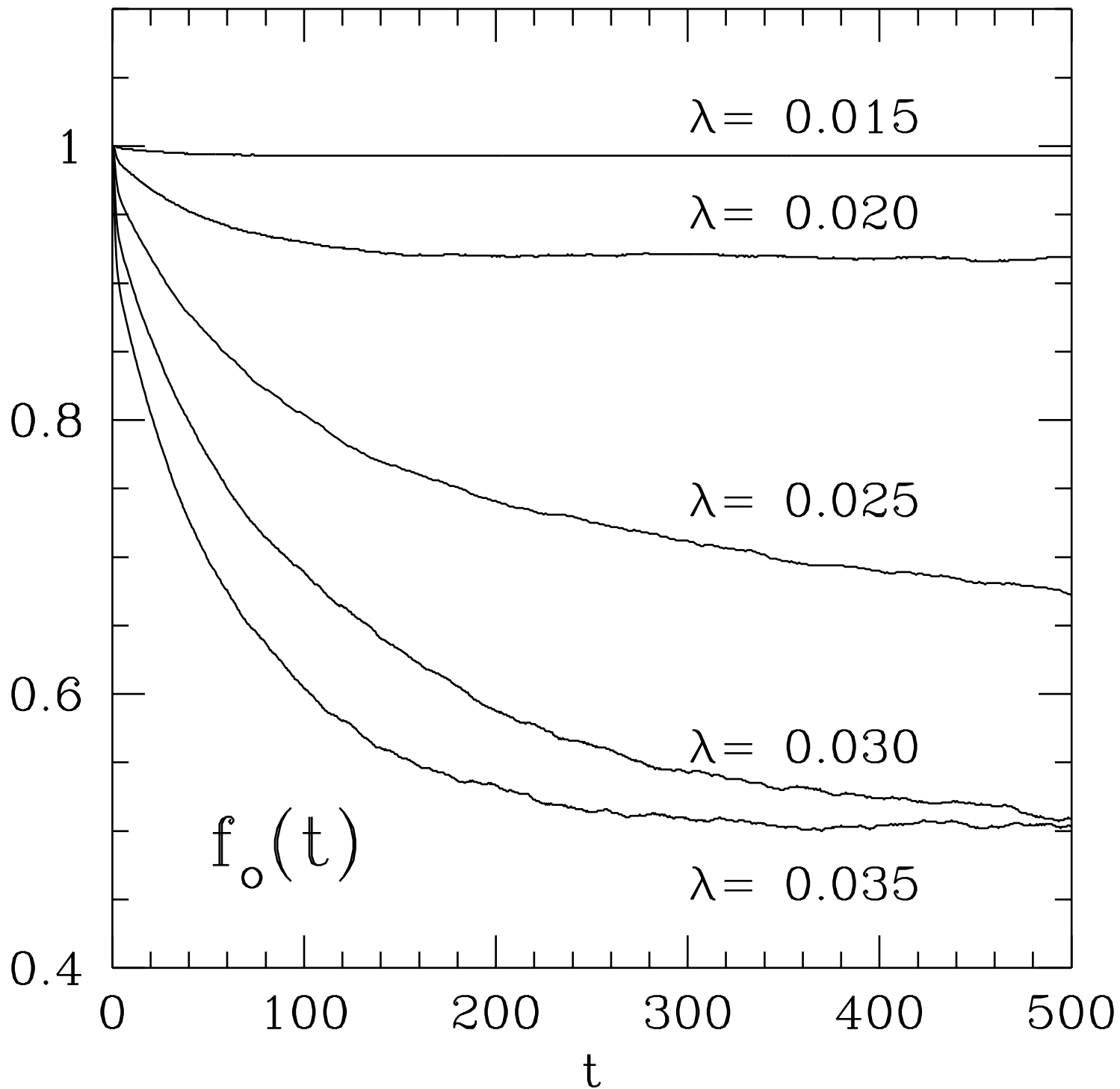
This figure "fig2-3.png" is available in "png" format from:

<http://arxiv.org/ps/hep-ph/9410235v2>



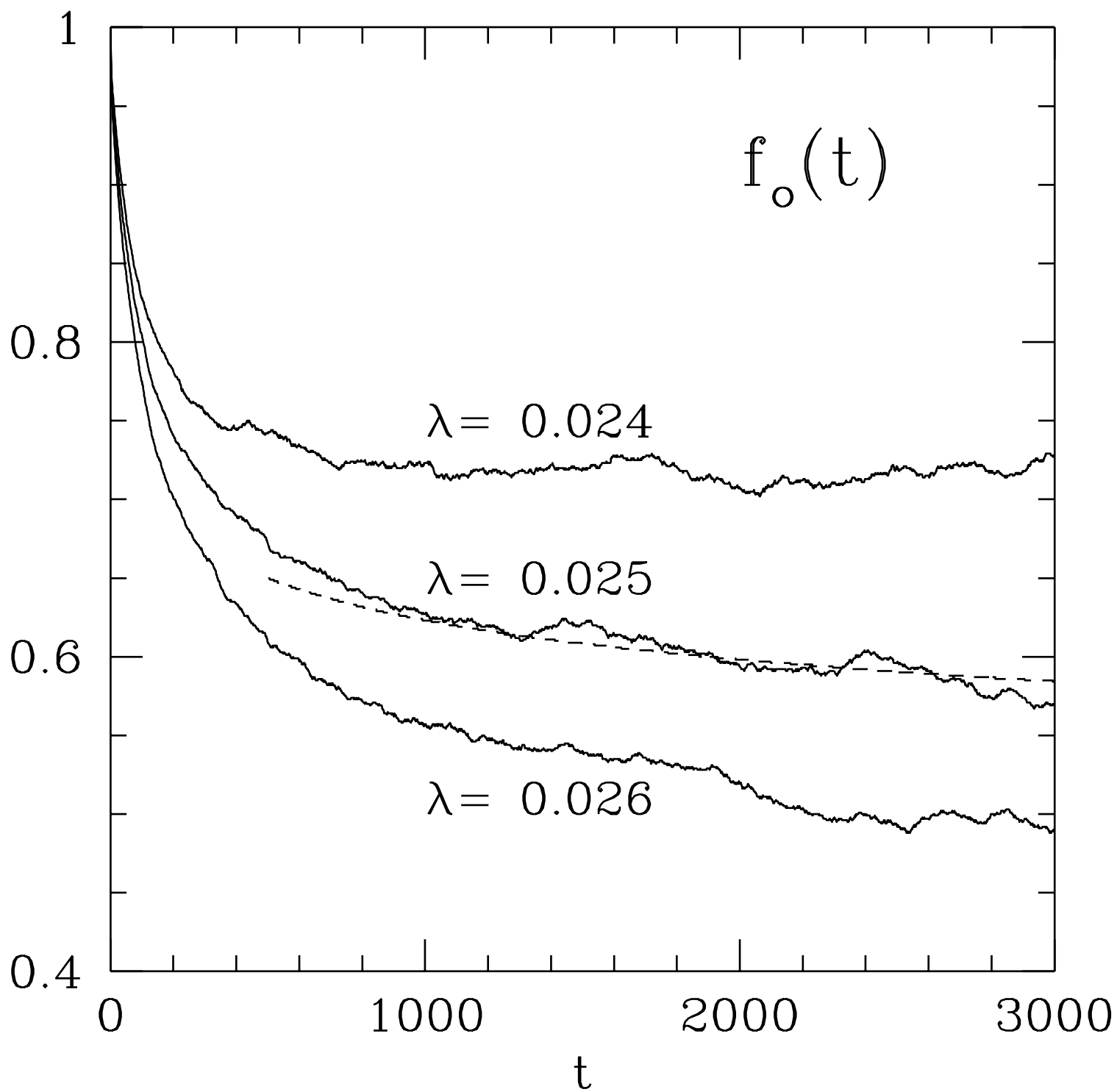
This figure "fig1-4.png" is available in "png" format from:

<http://arxiv.org/ps/hep-ph/9410235v2>



This figure "fig1-5.png" is available in "png" format from:

<http://arxiv.org/ps/hep-ph/9410235v2>



This figure "fig1-6.png" is available in "png" format from:

<http://arxiv.org/ps/hep-ph/9410235v2>

